Journal Pre-proof

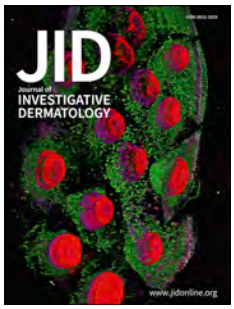

Lactate promotes collagen expression, proliferation and migration through H3K18 lactylation-dependent stimulation of LTBP3/TGF-β1 axis in keloid fibroblasts

Jing-Jing Gu, Cheng-Cheng Deng, Qing An, Ding-Heng Zhu, Xue-Yan Xu, Zheng-Zheng Fu, Zheng-Yang Zhou, Zhili Rong, Bin Yang

PII: S0022-202X(25)02245-6

DOI: https://doi.org/10.1016/j.jid.2025.04.044

Reference: JID 4883

To appear in: *The Journal of Investigative Dermatology*

Received Date: 23 April 2024

Revised Date: 1 April 2025

Accepted Date: 8 April 2025

Please cite this article as: Gu J-J, Deng C-C, An Q, Zhu D-H, Xu X-Y, Fu Z-Z, Zhou Z-Y, Rong Z, Yang B, Lactate promotes collagen expression, proliferation and migration through H3K18 lactylation-dependent stimulation of LTBP3/TGF-β1 axis in keloid fibroblasts, *Journal of Investigative Dermatology* (2025), doi: https://doi.org/10.1016/j.jid.2025.04.044.

Lactate promotes collagen expression, proliferation and migration through H3K18 lactylation-dependent stimulation of LTBP3/TGF-β1 axis in keloid fibroblasts

Jing-Jing Gu [# 1], Cheng-Cheng Deng [# 1], Qing An [3, 1], Ding-Heng Zhu [1], Xue-Yan Xu [1], Zheng-Zheng Fu [1], Zheng-Yang Zhou [1], Zhili Rong * [1, 2], Bin Yang * [1]

[1] Dermatology Hospital, Southern Medical University, Guangzhou, China.

[2] Cancer Research Institute, School of Basic Medical Sciences, State Key Laboratory of Multi-organ Injury Prevention and Treatment, Guangdong Province Key Laboratory of Immune Regulation and Immunotherapy, Southern Medical University, Guangzhou, China.

[3] The First School of Clinical Medicine, Southern Medical University, Guangzhou, China.

[#] Contributed equally.

[*] Contributed equally.

Correspondence: Bin Yang, Dermatology Hospital, Southern Medical University, Guangzhou 510091, China. Email: yangbin1@smu.edu.cn or Zhili Rong, Dermatology Hospital, Southern Medical University, Guangzhou 510091, China. E-mail: rongzhili@smu.edu.cn.

Tel: 86-20-83027645, Fax: 86-20-87255313

Keywords: Keloids; Histone lactylation; Collagen; Proliferation; Migration

Abstract

Keloids are fibroproliferative dermal lesions characterized by unrestrained fibroblast proliferation, collagen overproduction and persistent enlargement. Lactate has been suggested to regulate keloid fibroblast activity, although the underlying mechanism remains unclear. Histone lactylation is an important epigenetic regulatory mechanism by which lactate regulates pathophysiological processes, but its role in keloids remains to be studied. In this study, we discovered that the levels of pan-lysine lactylation (PanKla) and H3K18 lactylation were markedly increased in keloid fibroblasts (KFs) and that H3K18 lactylation mediated the positive effects of lactate on KF collagen expression, proliferation and migration. Furthermore, we found that lactate stimulated transforming growth factor-beta 1 (TGF-β1) secretion via H3K18 lactylation-dependent upregulation of LTBP3 transcription; in turn, TGF-β1 increased the lactate and H3K18 lactylation levels, possibly forming a positive feedback loop to continuously promote fibroblast collagen expression, proliferation and migration. Our data revealed that H3K18 lactylation plays a key role in KFs, elucidated the pathomechanisms underlying keloids and identified potential treatment targets.

Introduction

Keloids are fibroproliferative dermal lesions characterized by active fibroblast proliferation, excessive collagen accumulation, and persistent enlargement (Limandjaja et al., 2020). Keloids severely impact patients' quality of life due to pain, pruritus, cosmetic deformities, and restricted movement around the lesions (Andrews et al.,

2016). Genetics, epigenetics, hyperactive inflammation, and tension alignment have been proposed as factors involved in keloid pathogenesis in recent years (Deng et al., 2023, Liu et al., 2022). However, the mechanisms underlying keloid pathogenesis remain poorly understood, and effective treatments have not yet been discovered.

Fibroblasts are crucial in keloid pathogenesis (Deng et al., 2021). Increasing evidence suggests that keloid fibroblasts (KFs) undergo a metabolic switch from oxidative phosphorylation (OXPHOS) to aerobic glycolysis, leading to increased production of lactate (Su et al., 2022b, Vincent et al., 2008, Wang P. et al., 2023). Lactate, was previously viewed as metabolic waste, but it is now considered a multifunctional signaling molecule (Certo et al., 2022). Previous studies reported that blocking lactate can reduce KF proliferation, migration, and collagen expression, but the specific way in which lactate influences these processes is still unclear (Su et al., 2022a). Zhang et al. were the first to report that lactate can modify histones by attaching a lactyl group to histone lysine (K) residues, which is called “lactylation”, and this process is responsible for the epigenetic regulation of gene transcription (Zhang et al., 2019). Histone lactylation, a form of epigenetic alteration, has been described in studies on different illnesses, such as cancers (Yang et al., 2022, Yu et al., 2021), nervous system diseases (Pan et al., 2022, Wei et al., 2023), and fibrogenic responses (Li et al., 2022, Wang et al., 2024). However, whether and how histone lactylation regulates keloid fibroblasts remain unclear.

Our current research focused on evaluating the difference in histone lactylation levels between keloids and normal skin, as well as exploring the role of histone lactylation in KFs. Our findings suggested that the levels of lactate and H3K18 lactylation were markedly increased in KFs and that H3K18 lactylation mediated the positive effects of lactate on KF collagen expression, proliferation and migration. Mechanistically, lactate stimulates transforming growth factor-beta 1 (TGF-β1) secretion via H3K18 lactylation-dependent upregulation of LTBP3 transcription; in turn, TGF-β1 increases lactate and H3K18 lactylation levels, possibly forming a positive feedback loop to continuously promote KF collagen expression, proliferation and migration. These findings identify H3K18 lactylation as an epigenetic regulator that is dysregulated during keloid pathogenesis and provide a theoretical basis for the development of novel keloid treatment strategies.

Results

Histone lactylation levels are increased in keloids.

Given the metabolic reprogramming of KFs to switch from OXPHOS to glycolysis (Su et al., 2022b, Vincent et al., 2008), we evaluated lactate levels in keloids and normal skin. Colorimetric assays revealed that lactate levels were markedly elevated in keloid tissues (KTs) compared with those in normal skin tissues (NTs) (Figure 1a). Additionally, lactate levels were higher in KFs than in normal skin fibroblasts (NFs) (Figure 1b). As lactate is reported to serve as a precursor metabolite that is responsible for inducing histone lactylation (Zhang et al., 2019), we hypothesized that changes in

histone lactylation might occur in keloids. Western blotting analysis revealed notable increases in the levels of pan-lysine lactylation (PanKla), histone H3K18 lactylation (H3K18la), histone H3K14 lactylation (H3K14la), histone H4K16 lactylation (H4K16la), and histone H4K12 lactylation (H4K12la) (Figure 1c, 1d). As H3K18la was the most strongly increased among these forms of site-specific histone lactylation modifications (Figure 1d), we speculated that H3K18la is the primary form of histone lactylation in keloids. Furthermore, the protein expression intensity was evaluated by immunohistochemistry (IHC) and semiquantified according to an immunoreactive score (IRS) system as reported previously (Deng et al., 2019, Hu et al., 2017). The IHC results quantified by IRS analysis revealed that PanKla and H3K18la levels were markedly higher in KTs than in NTs (Figure 1e-g). Correlation analysis revealed a positive correlation between H3K18la and Pan Kla IRSs in clinical samples (Figure 1h). Moreover, a fibroblast marker (vimentin) was used for double-staining with PanKla or H3K18la (Sun et al., 2024), and the immunofluorescence (IF) results indicated that the percentages of PanKla+/Vimentin+ and H3K18la+/Vimentin+ cells among Vimentin-labeled cells were greater in KTs than in NTs (Supplementary Figure S1a, S1b). Together, these findings show that PanKla and H3K18 lactylation levels are notably increased in keloids compared with those in normal controls.

Lactate promotes keloid fibroblast collagen expression, proliferation, and migration with increased histone lactylation.

Keloids exhibit excessive collagen deposition (especially collagen-I and collagen-III

depositions), uncontrolled fibroblast proliferation, and active fibroblast migration (Andrews et al., 2016). To investigate the role of lactate and lactylation in KFs, we manipulated the overall levels of lactylation in KFs. In this study, lactate production and histone lactylation were hindered by a glycolytic inhibitor (oxamate) in KFs with high lactylation levels and enhanced by sodium lactate in KFs with low lactylation levels, as previously described (Yang et al., 2022, Zhang et al., 2019). Notably, oxamate significantly reduced the lactate concentration in KFs (Supplementary Figure S2a). Importantly, oxamate reduced collagen-I expression but not collagen-III expression in KFs (Supplementary Figure S2b, S2c). Additionally, oxamate significantly reduced PanKla and H3K18la levels in KFs (Supplementary Figure S2c). Furthermore, we found that oxamate significantly inhibited KF proliferation, as shown by Cell Counting Kit 8 (CCK-8) and 5-ethyl-2'-deoxyuridine (EdU) incorporation assays (Supplementary Figure S2d, S2e). Additionally, Transwell assays indicated that oxamate treatment blocked the migration of KFs (Supplementary Figure S2f). Furthermore, lactate treatment induced lactate production in KFs (Supplementary Figure S2g). Lactate had a significant effect on collagen-I expression but not collagen-III expression in KFs (Supplementary Figure S2h, S2i). Additionally, lactate significantly increased PanKla and H3K18la levels in KFs (Supplementary Figure S2i). Moreover, we discovered that lactate significantly stimulated KF proliferation, as shown by CCK-8 and EdU incorporation tests (Supplementary Figure S2j, S2k), and enhanced KF migration, as determined by Transwell assays (Supplementary Figure S2l). Collectively, our results reveal the pivotal role of lactate and lactylation in regulating

KFs.

H3K18 lactylation mediates the positive effects of lactate on collagen expression, proliferation, and migration in keloid fibroblasts.

We next further confirmed the role of H3K18 lactylation in modulating KFs. Previous studies reported that lysine (K)–to–arginine (R) mutation is used for mimicking the delactylated state of the protein (Fan et al., 2023, Yang et al., 2023). In this study, we mutated the lysine AAG codon to the arginine AGG codon and overexpressed the H3 wild type (WT) or H3K18R mutant in KFs with or without lactate treatment, respectively (Figure 2a). As shown in Figure 2c, H3K18la levels were decreased in H3K18R-mutated cells, and H3K18la levels were repressed in the lactate+H3K18R group compared with the lactate+H3WT group. Moreover, collagen-I expression was significantly lower in H3K18R-mutated cells than in H3WT cells, and the effect of lactate on collagen-I induction was abolished by H3K18 delactylation (Figure 2b, 2c). Proliferation was decreased in H3K18R-mutated cells, and the effect of lactate on KF proliferation was abolished by H3K18 delactylation (Figure 2d, 2e). Migration was decreased in H3K18R-mutated cells, and the effect of lactate on KF migration was abolished by H3K18 delactylation (Figure 2f). Overall, our findings reveal that H3K18 lactylation mediates the positive effects of lactate on collagen expression, proliferation, and migration in keloid fibroblasts.

H3K18 lactylation induces LTBP3 transcription in keloid fibroblasts.

Elevated histone lactylation can directly induce gene transcription and modulate macrophage polarization (Zhang et al., 2019), tumorigenesis (Yu et al., 2021), and microglial inflammation (Pan et al., 2022). Thus, we attempted to reveal how H3K18 lactylation regulates KFs via gene expression. We performed cleavage under targets and tagmentation followed by sequencing (CUT&Tag-seq) using anti-H3K18la antibodies. The CUT&Tag-seq results revealed that H3K18la was more abundant in promoter regions in KFs (27.87%) than in NFs (17.09%) (Figure 3a). Next, by combining CUT&Tag-seq data with RNA sequencing (RNA-seq) results for NFs and KFs, we identified 26 H3K18la target genes whose mRNA levels were significantly altered in KFs (Figure 3b). We identified the three genes with the greatest enrichment in the promoter regions (Figure 3b). Among the three genes, LTBP3 is related to collagen accumulation, cell proliferation, and migration according to published reports (Dabovic et al., 2005, Hou et al., 2017, Koli et al., 2008, Robertson and Rifkin, 2016), and according to both the CUT&Tag-seq and RNA-seq analyses, its expression was more strongly altered in KFs than in NFs; therefore, we focused on this gene. Using IGV software, we detected a significant increase in H3K18la signal enrichment in the LTBP3 promoter among KFs compared with NFs (Figure 3c). Similarly, there was a notable increase in LTBP3 levels in KFs compared NFs (Figure 3d). Moreover, the CUT&Tag-qPCR results revealed a marked increase in H3K18la levels within the LTBP3 promoter in KFs compared with NFs (Figure 3e). Consistent with this, qPCR and Western blotting analysis revealed a significant increase in LTBP3 levels in KFs (Figure 3f, 3g). The IHC results quantified by IRS analysis revealed that LTBP3 expression was

significantly higher in KTs than in NTs (Figure 3h), and Correlation analysis suggested that H3K18la levels were positively correlated with LTBP3 levels in clinical samples (Figure 3i). The IF results revealed that the proportion of LTBP3+/Vimentin+ cells among Vimentin-labeled cells was higher in KTs than in NTs (Supplementary Figure S1c). Moreover, CUT&Tag-qPCR analysis revealed a notable reduction in H3K18la levels within the LTBP3 promoter in KFs treated with oxamate (Figure 3j), and there was a significant reduction in LTBP3 expression in KFs treated with oxamate (Figure 3k, 3l). Furthermore, CUT&Tag-qPCR analysis revealed a notable reduction in H3K18la levels within the LTBP3 promoter in H3K18R-mutated KFs, and the effect of lactate on H3K18la levels within the LTBP3 promoter was abolished by H3K18 delactylation (Figure 3m). Consistent with this, there was a marked reduction in LTBP3 expression in H3K18R-mutated KFs, and the effect of lactate on LTBP3 expression was abolished by H3K18 delactylation (Figure 3n, 3o). Overall, these findings suggest that lactate induces LTBP3 transcription through H3K18 lactylation.

Lactate enhances collagen expression, proliferation, and migration via H3K18la-dependent induction of LTBP3 in keloid fibroblasts.

We subsequently aimed to explore the biological function of LTBP3 in KFs. Two small interfering RNAs (siRNAs) that target LTBP3 were designed and delivered into KFs to develop a cell model with reduced LTBP3 levels. The effectiveness of the siRNAs in decreasing LTBP3 levels was confirmed through qPCR and Western blotting analysis (Figure 4a, 4b). The expression of collagen-I was substantially reduced after LTBP3

knockdown, and the effect of lactate on collagen-I induction was abrogated by LTBP3 siRNA transfection (Figure 4a, 4b). Additionally, the proliferation of KFs was suppressed after LTBP3 knockdown, and the influence of lactate on KF proliferation was abolished via LTBP3 siRNA transfection (Figure 4c, 4d). Furthermore, there was a notable decrease in the migration of KFs after LTBP3 knockdown, and the impact of lactate on KF migration was eliminated through LTBP3 siRNA transfection (Figure 4e). These results indicate that lactate promotes KF collagen expression, proliferation, and migration via H3K18la-independent induction of LTBP3.

LTBP3 promotes collagen expression, proliferation, and migration through TGF-β1 in keloid fibroblasts.

LTBP3 is critical for the secretion, maturation, and function of TGF-β1 (Deryugina et al., 2018, Robertson et al., 2015), and TGF-β1 is considered one of the principal cytokines that contributes to keloid pathogenesis (Hu et al., 2017, Macarak et al., 2021). Thus, we wondered whether TGF-β1 mediates the promoting effect of LTBP3 on the regulation of KF. In addition, collagen-I expression was suppressed in KFs after LTBP3 knockdown (Supplementary Figure S3a, S3b). Moreover, the proliferation of KFs was suppressed after LTBP3 knockdown (Supplementary Figure S3c, S3d). The migration of KFs was significantly inhibited after LTBP3 knockdown (Supplementary Figure S3e). These effects of LTBP3 siRNA could be markedly diminished by the exogenous application of recombinant TGF-β1 (Supplementary Figure S3a-e). Together, our findings reveal that LTBP3 enhances KF collagen production, proliferation, and

migration through TGF-β1.

Lactate potentiates collagen expression, proliferation, and migration through H3K18la/LTBP3-dependent induction of TGF-β1 secretion in keloid fibroblasts.

We next sought to investigate whether TGF-β1 mediates the positive effect of lactate on KF regulation. The ELISA results suggested that oxamate treatment significantly decreased the TGF-β1 levels in KFs (Figure 5a). There was a marked increase in TGF-β1 levels in KFs treated with lactate, and this effect was significantly diminished in H3K18R-mutated cells (Figure 5b). Moreover, we observed a notable reduction in TGF-β1 levels following LTBP3 knockdown in KFs, and the effect of lactate on TGF-β1 activation was nullified through LTBP3 siRNA transfection (Figure 5c). Herein, the pan-TGF-β neutralizing antibody 1D11 was utilized to antagonize TGF-β1 (Dasch et al., 1989, Li et al., 2023). The expression of collagen-I was markedly inhibited in KFs that were treated with 1D11, and the effect of lactate on collagen-I induction was abolished by 1D11 treatment (Figure 5d, 5e). The proliferation of KFs treated with 1D11 decreased, and the effect of lactate on KF proliferation was abolished through 1D11 treatment (Figure 5f, 5g). Furthermore, there was a notable reduction in the migration of KFs treated with 1D11, and the effect of lactate on KF migration was eliminated via 1D11 treatment (Figure 5h). Together, our findings reveal that lactate promotes KF collagen expression, proliferation, and migration through H3K18la/LTBP3-dependent induction of TGF-β1 secretion.

TGF-β1 increases lactate and H3K18 lactylation levels in keloid fibroblasts.

TGF-β1 has been reported to stimulate glycolysis and lactate production in cancer cells (Hua et al., 2020) and lung fibroblasts (Wang W. et al., 2023); therefore, we questioned whether TGF-β1 alters the levels of lactate and histone lactylation in KFs. Colorimetric assays revealed a notable reduction in lactate levels in KFs treated with 1D11(Figure 6a). Moreover, there were notable decreases in the levels of PanKla, H3K18la, and collagen-I in KFs after 1D11 treatment (Figure 6b). Additionally, recombinant TGF-β1 induced lactate production and increased PanKla, H3K18la, and collagen-I levels in KFs (Figure 6c, 6d). These results demonstrate that TGF-β1 stimulates histone lactylation, indicating the existence of a positive feedback loop between H3K18 lactylation and TGF-β1.

Discussion

Keloids are fibroproliferative dermal lesions that are unique to humans, and usually occur due to unnatural wound healing (Fujita et al., 2019). Keloids exhibit uncontrolled growth extending beyond the original wound margins through dysregulated fibroblast proliferation, enhanced migratory activity, and excessive deposition of collagen fibers (Macarak et al., 2021). To date, the mechanisms underlying abnormal fibroblast biological features during keloid pathogenesis have not been fully elucidated. Here, we found that H3K18 lactylation was significantly increased in keloids, indicating that the lactate/H3K18la/LTBP3/TGF-β1 positive feedback loop is part of a crucial mechanism underlying the abnormal biological behavior of KFs (Figure 6e). These findings reveal

that disrupting this detrimental cycle of reinforcement could be a promising approach for keloid treatment.

Histone lactylation is a crucial process that links metabolism and epigenetics by directly inducing gene transcription (Xin et al., 2022). Emerging evidence has shown that histone lactylation is involved in fibrous diseases, including idiopathic pulmonary fibrosis (Wang et al., 2024), liver fibrosis (Rho et al., 2023), and placental fibrosis (Li et al., 2022). Epigenetic factors are considered important in keloid pathogenesis (Lv et al., 2020, Nyika et al., 2022, Stevenson et al., 2021). To our knowledge, the role of histone lactylation in keloid pathogenesis remains unexplored. Despite previous research demonstrating that blocking lactate can reduce KF proliferation, migration, and collagen expression, the specific way in which lactate influences these processes is still unclear (Su et al., 2022a). Our study revealed elevated levels of PanKla and H3K18 lactylation in keloids, consistent with previous research indicating the accumulation of lactate, the precursor of lactylation, in keloids (Su et al., 2022b, Vincent et al., 2008). Furthermore, lactate stimulated TGF-β1 secretion via H3K18 lactylation-dependent upregulation of LTBP3 transcription; in turn, TGF-β1 enhanced lactate and H3K18 lactylation, thereby forming a positive feedback loop to continuously promote KF collagen expression, proliferation, and migration. These findings highlight a function of histone lactylation and extend the mechanistic understanding of lactate-induced abnormal biological behavior of KFs. Overall, the essential metabolic-epigenetic cascade presented in our study provides insights into the pathomechanisms underlying

keloids and offers promising targets for keloid treatment. Additionally, there may exist other pathways through which lactate regulates KFs, not just H3K18 lactylation. We hope that our subsequent research can clarify this, thereby better understanding the pathophysiology of keloids.

Our research revealed that LTBP3 mediates the effect of H3K18 lactylation on promoting fibroblast collagen expression, proliferation, and migration. As a member of the LTBP family, LTBP3 can covalently bind to TGF-β1 and is required for the accurate folding, secretion, and function of TGF-β1 (Deryugina et al., 2018, Hou et al., 2017, Robertson and Rifkin, 2016). In the rough endoplasmic reticulum, an LTBP molecule covalently binds to the pro-TGF-β homodimer (latency-associated peptide, LAP), forming a large latent complex (LLC). Proper TGF-β function relies on LLC formation, which can be hindered by mutating the binding cysteine residues in either LTBP or LAP, leading to the obstruction of latent TGF-β activation (Singh et al., 2022). Without LTBP, incorrect disulfide bonds may form between the cysteines in LAP that bind to LTBP, resulting in the degradation of LAP within cells (Brunner et al., 1989). This could explain the increased secretion of TGF-β when LTBP is present (Rifkin, 2005, Robertson and Rifkin, 2016). LTBP-1 and LTBP-3 can effectively bind with LAP, which includes any of the three TGF-β isoforms (Deryugina et al., 2018). Research has indicated that LTBP3 plays a role in bone disorders (Dabovic et al., 2005, Koli et al., 2008), cancers (Deryugina et al., 2018, Hou et al., 2017), and adipogenesis (Singh et al., 2022). Nevertheless, the impact of LTBP3 on the advancement of keloids remains

uninvestigated. Our research revealed that LTBP3 expression was increased in keloids, that LTBP3 was a direct target of H3K18 lactylation, and that LTBP3 acted as an important mediator of lactate, activating TGF-β1 to facilitate KF collagen expression, proliferation, and migration. This work expands research on LTBP3 in different contexts and illustrates the essential role of LTBP3 in KF regulation; our findings indicate that LTBP3 may be a promising biomarker or target in keloids.

TGF-β1, a well-researched cytokine, plays a crucial role in the etiopathogenesis of keloids (Limandjaja et al., 2020). Overwhelming evidence has shown that TGF-β1 performs pluripotent biological functions, ranging from functions related to proliferation to those related to cellular plasticity, by activating downstream signaling pathways, including the SMAD and Wnt complex signaling pathways, in various conditions and disease states, including keloids (Andrews et al., 2016). Previous studies have reported that TGF-β1 can increase glycolysis and upregulate key glycolytic factors (such as GLUT1 and PFKFB3) in hepatic stellate cells and glioblastoma cells by activating the Smad, p38 MAPK and P13K/AKT signaling pathways (Rodríguez-García et al., 2017, Zhou et al., 2021), suggesting that TGF-β1 may induce histone lactylation. Our research revealed that elevated histone lactylation induced TGF-β1 secretion; interestingly, TGF-β1, in turn, increased lactate and histone lactylation levels in KFs. These findings reveal crosstalk among metabolism, epigenetics, and cytokines, indicating that there exist sophisticated and complex mechanisms of cell regulation in keloids. We speculate that owing to the presence of the self-amplified loop, keloids

exhibit sustained growth and are fundamentally distinct from common scars. Additional experiments are needed to test this hypothesis.

With technological development, several histone lactylation-specific sites, such as H3K18, H3K9, H4K12, and H4K8, have been identified; among these sites, H3K18 was the first to be reported and is the most extensively studied (Galle et al., 2022, Wang et al., 2024, Wei et al., 2023, Zhang et al., 2019).To our knowledge, no study has identified H3K18la as a key regulator of KF collagen expression, proliferation and migration. Our study revealed that H3K18la/LTBP3/TGF-β1 forms a positive feedback loop and that inhibition of this loop impaired KF collagen expression, proliferation, and migration. However, whether other site-specific histone lactylation or nonhistone protein lactylation modifications are involved in keloid pathogenesis remains unclear. This question will be explored further.

In summary, we found that the PanKla and H3K18 lactylation levels were significantly increased in keloids and that H3K18 lactylation mediated the positive effects of lactate on KF collagen expression, proliferation and migration. Mechanistically, lactate stimulates TGF-β1 secretion via H3K18 lactylation-dependent upregulation of LTBP3 transcription; in turn, TGF-β1 increases lactate and H3K18 lactylation levels, possibly forming a positive feedback loop to continuously promote fibroblast collagen expression, proliferation and migration. Our data suggest that H3K18 lactylation plays a key role in KFs, and these discoveries will aid in understanding the pathomechanisms

of keloids and identifying prospective targets for keloid therapies.

Materials and methods

Sample collection

This research was authorized by the Medical and Ethics Committees of Dermatology Hospital, Southern Medical University. Before joining this study, each subject signed a written informed consent form. Normal skin samples were obtained from the skin adjacent to the removed benign pigment nevi or the removed normal skin during aesthetic plastic surgery (such as abdominoplasty) in healthy volunteers. Keloid samples were obtained from patients who were diagnosed with keloids through histopathology and who had not undergone any physical or medical interventions before surgical removal. Donor information is provided in Supplementary Table S1.

Cell culture

Fresh tissues were used to isolate primary fibroblasts following established methods (Hu et al., 2014, Tang et al., 2011). These cells were then cultured in high-glucose Dulbecco's modified Eagle's medium (Gibco, Carlsbad, CA) supplemented with 10% fetal bovine serum (Corning, NY, USA) and maintained at 37°C in a 5% CO_2 environment. Fibroblasts at passages 4 to 6 were used for experiments. Certain cells were treated with oxamate (Selleckchem, Houston, USA), lactate (Sigma–Aldrich, St. Louis, USA), 1D11 (R&D Systems, Minneapolis, MN), or recombinant human TGF-β1 (R&D Systems).

Cleavage under targets and tagmentation (CUT&Tag) assay

The CUT&Tag assay was carried out with a Hieff NGS® G-Type In Situ DNA Binding Profiling Library Prep Kit for Illumina (Yeasen Bio, Shanghai, China) following the manufacturer's protocols. In brief, fibroblasts were harvested and bound to activated concanavalin A-coated magnetic beads. Then, the cells that had been resuspended were incubated with an antibody against H3K18la (PTM Bio, PTM-1427RM) for 2 h at 37°C under gently rotation. The secondary antibody was subsequently added, and the mixture was incubated at 37°C with gentle rotation for 1 h. After washing, the pA/G-Tn5 transposase was added, and then proteinase K was added. After extraction, amplification, and purification, the DNA was subjected to sequencing and qPCR.

Statistical analysis

The data are presented as the means ± standard deviations, with each experiment being conducted independently a minimum of three times independently. Statistical analysis was conducted with the software program GraphPad Prism version 8.0.2 (GraphPad, La Jolla, CA). An unpaired t test or one-way analysis of variance was used to examine the statistical significance of the differences, and $P<0.05$ was considered indicative of statistical significance.

Data availability statement

The primary information backing the crucial findings of the research can be found in

this paper and its Supplementary Materials and Methods. The raw CUT&Tag-seq and RNA-seq data used in this study have been deposited in the Genome Sequence Archive for Human repository of the National Genomics Data Center (https://ngdc.cncb.ac.cn/gsa-human), under accession numbers HRA008369 and HRA008366, respectively. The sequencing data accession numbers (HRA008369 and HRA008366) referenced in this study were submitted to this Journal on May 20, 2025.

ORCIDs

Jing-Jing Gu: https://orcid.org/0000-0002-8934-3792

Cheng-Cheng Deng: https://orcid.org/0000-0001-9616-1607

Qing An: https://orcid.org/0000-0001-8959-2652

Ding-Heng Zhu: https://orcid.org/0000-0003-4972-4635

Xue-Yan Xu: https://orcid.org/0000000269805654

Zheng-Zheng Fu: https://orcid.org/0009-0003-6895-3123

Zheng-Yang Zhou: https://orcid.org/ 0000-0001-6654-0462

Zhili Rong: https://orcid.org/0000-0002-1699-7074

Bin Yang: https://orcid.org/0000-0002-7155-6079

Conflict of interest

There are no conflicts of interest.

Acknowledgments

This work was supported by the National Natural Science Foundation of China (82303981, 82373457), the China Postdoctoral Science Foundation (2023M741566) and the Natural Science Foundation of Guangdong Province (2023A1515010120). We sincerely thank Haoyu Xie, Jun Liu, Yan Zhang, Yingping Xu and Yongjun Zhang for worthwhile scientific discussions. Bin Yang will act as the guarantor of this article.

Author contributions

Conceptualization: BY, JJG; Funding acquisition: JJG, BY, CCD; Data curation: JJG, CCD; Formal analysis: JJG, CCD; Methodology: ZR, JJG, CCD; Investigation: JJG, CCD, QA, DHZ, XYX, ZZF, ZYZ; Resources: BY, DHZ; Software: JJG, QA; Supervision: BY, ZR; Writing-Original Draft Preparation: JJG, BY; Writing-Review and Editing: BY, ZR, CCD.

References

Andrews JP, Marttala J, Macarak E, Rosenbloom J, Uitto J. Keloids: The paradigm of skin fibrosis - Pathomechanisms and treatment. Matrix Biol 2016;51:37-46.

Brunner AM, Marquardt H, Malacko AR, Lioubin MN, Purchio AF. Site-directed mutagenesis of cysteine residues in the pro region of the transforming growth factor beta 1 precursor. Expression and characterization of mutant proteins. J Biol Chem 1989;264(23):13660-4.

Certo M, Llibre A, Lee W, Mauro C. Understanding lactate sensing and signalling. Trends Endocrinol Metab 2022;33(10):722-35.

Dabovic B, Levasseur R, Zambuto L, Chen Y, Karsenty G, Rifkin DB. Osteopetrosis-like phenotype in latent TGF-beta binding protein 3 deficient mice. Bone 2005;37(1):25-31.

Dasch JR, Pace DR, Waegell W, Inenaga D, Ellingsworth L. Monoclonal antibodies recognizing transforming growth factor-beta. Bioactivity neutralization and transforming growth factor beta 2 affinity purification. J Immunol 1989;142(5):1536-41.

Deng C, Zhu D, Chen Y, Huang T, Peng Y, Liu S, et al. TRAF4 Promotes Fibroblast Proliferation in Keloids by Destabilizing p53 via Interacting with the Deubiquitinase USP10. The Journal of investigative dermatology 2019;139(9):1925-35.e5.

Deng CC, Hu YF, Zhu DH, Cheng Q, Gu JJ, Feng QL, et al. Single-cell RNA-seq reveals fibroblast

heterogeneity and increased mesenchymal fibroblasts in human fibrotic skin diseases. Nat Commun 2021;12(1):3709.

Deng CC, Zhang LX, Xu XY, Zhu DH, Cheng Q, Ma S, et al. Risk single-nucleotide polymorphism-mediated enhancer-promoter interaction drives keloids through long noncoding RNA down expressed in keloids. Br J Dermatol 2023;188(1):84-93.

Deryugina EI, Zajac E, Zilberberg L, Muramatsu T, Joshi G, Dabovic B, et al. LTBP3 promotes early metastatic events during cancer cell dissemination. Oncogene 2018;37(14):1815-29.

Fan W, Wang X, Zeng S, Li N, Wang G, Li R, et al. Global lactylome reveals lactylation-dependent mechanisms underlying T(H)17 differentiation in experimental autoimmune uveitis. Sci Adv 2023;9(42):eadh4655.

Fujita M, Yamamoto Y, Jiang JJ, Atsumi T, Tanaka Y, Ohki T, et al. NEDD4 Is Involved in Inflammation Development during Keloid Formation. J Invest Dermatol 2019;139(2):333-41.

Galle E, Wong CW, Ghosh A, Desgeorges T, Melrose K, Hinte LC, et al. H3K18 lactylation marks tissue-specific active enhancers. Genome Biol 2022;23(1):207.

Hou Z, Xu X, Fu X, Tao S, Zhou J, Liu S, et al. HBx-related long non-coding RNA MALAT1 promotes cell metastasis via up-regulating LTBP3 in hepatocellular carcinoma. Am J Cancer Res 2017;7(4):845-56.

Hu ZC, Shi F, Liu P, Zhang J, Guo D, Cao XL, et al. TIEG1 Represses Smad7-Mediated Activation of TGF-β1/Smad Signaling in Keloid Pathogenesis. J Invest Dermatol 2017;137(5):1051-9.

Hu ZC, Tang B, Guo D, Zhang J, Liang YY, Ma D, et al. Expression of insulin-like growth factor-1 receptor in keloid and hypertrophic scar. Clin Exp Dermatol 2014;39(7):822-8.

Hua W, Ten Dijke P, Kostidis S, Giera M, Hornsveld M. TGFβ-induced metabolic reprogramming during epithelial-to-mesenchymal transition in cancer. Cell Mol Life Sci 2020;77(11):2103-23.

Koli K, Ryynänen MJ, Keski-Oja J. Latent TGF-beta binding proteins (LTBPs)-1 and -3 coordinate proliferation and osteogenic differentiation of human mesenchymal stem cells. Bone 2008;43(4):679-88.

Li X, Yang N, Wu Y, Wang X, Sun J, Liu L, et al. Hypoxia regulates fibrosis-related genes via histone lactylation in the placentas of patients with preeclampsia. J Hypertens 2022;40(6):1189-98.

Li Y, Wang X, Hu B, Sun Q, Wan M, Carr A, et al. Neutralization of excessive levels of active TGF-β1 reduces MSC recruitment and differentiation to mitigate peritendinous adhesion. Bone Res 2023;11(1):24.

Limandjaja GC, Niessen FB, Scheper RJ, Gibbs S. The Keloid Disorder: Heterogeneity, Histopathology, Mechanisms and Models. Front Cell Dev Biol 2020;8:360.

Liu S, Yang H, Song J, Zhang Y, Abualhssain ATH, Yang B. Keloid: Genetic susceptibility and contributions of genetics and epigenetics to its pathogenesis. Exp Dermatol 2022;31(11):1665-75.

Lv W, Ren Y, Hou K, Hu W, Yi Y, Xiong M, et al. Epigenetic modification mechanisms involved in keloid: current status and prospect. Clin Epigenetics 2020;12(1):183.

Macarak EJ, Wermuth PJ, Rosenbloom J, Uitto J. Keloid disorder: Fibroblast differentiation and gene expression profile in fibrotic skin diseases. Exp Dermatol 2021;30(1):132-45.

Nyika DT, Khumalo NP, Bayat A. Genetics and Epigenetics of Keloids. Adv Wound Care (New Rochelle) 2022;11(4):192-201.

Pan RY, He L, Zhang J, Liu X, Liao Y, Gao J, et al. Positive feedback regulation of microglial glucose metabolism by histone H4 lysine 12 lactylation in Alzheimer's disease. Cell Metab

2022;34(4):634-48.e6.

Rho H, Terry AR, Chronis C, Hay N. Hexokinase 2-mediated gene expression via histone lactylation is required for hepatic stellate cell activation and liver fibrosis. Cell Metab 2023;35(8):1406-23.e8.

Rifkin DB. Latent transforming growth factor-beta (TGF-beta) binding proteins: orchestrators of TGF-beta availability. J Biol Chem 2005;280(9):7409-12.

Robertson IB, Horiguchi M, Zilberberg L, Dabovic B, Hadjiolova K, Rifkin DB. Latent TGF-β-binding proteins. Matrix Biol 2015;47:44-53.

Robertson IB, Rifkin DB. Regulation of the Bioavailability of TGF-β and TGF-β-Related Proteins. Cold Spring Harb Perspect Biol 2016;8(6).

Rodríguez-García A, Samsó P, Fontova P, Simon-Molas H, Manzano A, Castaño E, et al. TGF-β1 targets Smad, p38 MAPK, and PI3K/Akt signaling pathways to induce PFKFB3 gene expression and glycolysis in glioblastoma cells. Febs j 2017;284(20):3437-54.

Singh K, Sachan N, Ene T, Dabovic B, Rifkin D. Latent transforming growth factor β binding protein 3 controls adipogenesis. Matrix Biol 2022;112:155-70.

Stevenson AW, Deng Z, Allahham A, Prêle CM, Wood FM, Fear MW. The epigenetics of keloids. Exp Dermatol 2021;30(8):1099-114.

Su Z, Fan J, Liu L, Jiao H, Tian J, Gan C, et al. Inhibiting Warburg Effect Can Suppress the Biological Activity and Secretion Function of Keloid Fibroblasts. Aesthetic Plast Surg 2022a;46(4):1964-72.

Su Z, Jiao H, Fan J, Liu L, Tian J, Gan C, et al. Warburg effect in keloids: A unique feature different from other types of scars. Burns 2022b;48(1):176-83.

Sun J, Jia W, Qi H, Huo J, Liao X, Xu Y, et al. An Antioxidative and Active Shrinkage Hydrogel Integratedly Promotes Re-Epithelization and Skin Constriction for Enhancing Wound Closure. Adv Mater 2024;36(21):e2312440.

Tang B, Zhu B, Liang Y, Bi L, Hu Z, Chen B, et al. Asiaticoside suppresses collagen expression and TGF-β/Smad signaling through inducing Smad7 and inhibiting TGF-βRI and TGF-βRII in keloid fibroblasts. Arch Dermatol Res 2011;303(8):563-72.

Vincent AS, Phan TT, Mukhopadhyay A, Lim HY, Halliwell B, Wong KP. Human skin keloid fibroblasts display bioenergetics of cancer cells. J Invest Dermatol 2008;128(3):702-9.

Wang P, Wang Q, Yang X, An Y, Wang J, Nie F, et al. Targeting the glycolytic enzyme PGK1 to inhibit the Warburg effect: a new strategy for keloid therapy. Plast Reconstr Surg 2023.

Wang P, Xie D, Xiao T, Cheng C, Wang D, Sun J, et al. H3K18 lactylation promotes the progression of arsenite-related idiopathic pulmonary fibrosis via YTHDF1/m6A/NREP. J Hazard Mater 2024;461:132582.

Wang W, Zhang Y, Huang W, Yuan Y, Hong Q, Xie Z, et al. Alamandine/MrgD axis prevents TGF-β1-mediated fibroblast activation via regulation of aerobic glycolysis and mitophagy. J Transl Med 2023;21(1):24.

Wei L, Yang X, Wang J, Wang Z, Wang Q, Ding Y, et al. H3K18 lactylation of senescent microglia potentiates brain aging and Alzheimer's disease through the NFκB signaling pathway. J Neuroinflammation 2023;20(1):208.

Xin Q, Wang H, Li Q, Liu S, Qu K, Liu C, et al. Lactylation: a Passing Fad or the Future of Posttranslational Modification. Inflammation 2022;45(4):1419-29.

Yang J, Luo L, Zhao C, Li X, Wang Z, Zeng Z, et al. A Positive Feedback Loop between Inactive VHL-Triggered Histone Lactylation and PDGFRβ Signaling Drives Clear Cell Renal Cell Carcinoma

Progression. Int J Biol Sci 2022;18(8):3470-83.

Yang Z, Yan C, Ma J, Peng P, Ren X, Cai S, et al. Lactylome analysis suggests lactylation-dependent mechanisms of metabolic adaptation in hepatocellular carcinoma. Nat Metab 2023;5(1):61-79.

Yu J, Chai P, Xie M, Ge S, Ruan J, Fan X, et al. Histone lactylation drives oncogenesis by facilitating m(6)A reader protein YTHDF2 expression in ocular melanoma. Genome Biol 2021;22(1):85.

Zhang D, Tang Z, Huang H, Zhou G, Cui C, Weng Y, et al. Metabolic regulation of gene expression by histone lactylation. Nature 2019;574(7779):575-80.

Zhou MY, Cheng ML, Huang T, Hu RH, Zou GL, Li H, et al. Transforming growth factor beta-1 upregulates glucose transporter 1 and glycolysis through canonical and noncanonical pathways in hepatic stellate cells. World J Gastroenterol 2021;27(40):6908-26.

Figure legends

Figure 1. Histone lactylation levels are increased in keloids. (a) Colorimetric assays measuring lactate levels in NTs and KTs (n=12 per group). (b) Colorimetric assays measuring lactate levels in NFs and KFs (n=12 per group). (c) Western blotting analysis of pan- and site-specific histone lactylation in NFs and KFs (n=5 per group). (d) Quantification of the data in (c). (e, f) Representative immunohistochemical images of PanKla in NTs and KTs (n=10 per group), with quantification using IRS analysis. Bar: 100 μm. (g) Representative immunohistochemical images of H3K18la in NTs and KTs (n=10 per group), with quantification using IRS analysis. Bar: 100 μm. (h) Correlation analysis of the IRS between H3K18la and PanKla in NTs and KTs. *$P<0.05$, **$P<0.01$, ***$P<0.001$. IRS, immunoreactive score; KF, keloid fibroblast; KT, keloid tissue; NF, normal skin fibroblast; ns, not significant; NT, normal skin tissue.

Figure 2. H3K18 lactylation mediates the positive effects of lactate on collagen expression, proliferation, and migration in keloid fibroblasts. (a) Overlap PCR was used for the construction of the mutation plasmid. Sanger sequencing was used to verify

whether lysine (AAG) was mutated to arginine (AGG). (b) The mRNA levels of COL1A1 and COL1A2 in KFs overexpressing H3 or its K18R mutant following lactate (20 mM) treatment. (c) Western blotting analysis of collagen-I and H3K18la in KFs overexpressing H3 or its K18R mutant following lactate (20 mM) treatment. (d, e) The proliferation of KFs overexpressing H3 or its K18R mutant following lactate (20 mM) treatment was evaluated using CCK-8 and EdU incorporation assays. The brightness and contrast were adjusted uniformly within each channel. Bar: 200 μm. (f) The migration of KFs overexpressing H3 or its K18R mutant following lactate (20 mM) treatment was evaluated using Transwell assay. Bar: 200 μm. *$P<0.05$, ***$P<0.001$. CCK-8, Cell Counting Kit 8; EdU, 5-ethynyl-2'-deoxyuridine; h, hour; KF, keloid fibroblast; mM, mmol/L; ns, not significant; OD, optical density.

Figure 3. H3K18 lactylation induces LTBP3 transcription in keloid fibroblasts. (a) Genome-wide distribution of H3K18la-binding peaks in NFs and KFs. (b) Venn diagram analysis of the CUT&Tag-seq and RNA-seq data of KFs and NFs. (c) Representative IGV tracks showing enrichment of H3K18la modifications in the LTBP3 promoter according to CUT&Tag-seq. The red rectangle indicates the peak region of H3K18la in the LTBP3 promoter. (d) Representative IGV tracks showing increased LTBP3 expression in KFs according to RNA-seq. (e) CUT&Tag-qPCR was used to analyze the enrichment of H3K18la on the LTBP3 promoter in NFs and KFs. (f) The mRNA levels of LTBP3 in NFs and KFs were assessed by qPCR (n=9 per group). (g) The protein expression of LTBP3 in NFs and KFs (n=5 per group). (h)

Representative immunohistochemical images of LTBP3 in normal skin and keloids (n=10 per group), with quantification using IRS analysis. Bar: 100 μm. (i) Correlation analysis of the IRS between H3K18la (Figure 1f) and LTBP3 in normal skin and keloids. (j) CUT&Tag-qPCR analysis for the enrichment of H3K18la on the LTBP3 promoter in KFs that were treated with oxamate (20 mM) for 24 h. (k, l) The mRNA and protein levels of LTBP3 in KFs treated with oxamate (0-20 mM) were evaluated using qPCR and Western blotting for 48 h. (m) CUT&Tag-qPCR analysis for the enrichment of H3K18la on the LTBP3 promoter in KFs overexpressing H3 or its K18R mutant following lactate (20 mM) treatment. (n, o) The mRNA and protein levels of LTBP3 in KFs overexpressing H3 or its K18R mutant following lactate (20 mM) treatment. *$P<0.05$, **$P<0.01$, ***$P<0.001$. h, hour; IRS, immunoreactive score; KF, keloid fibroblast; mM, mmol/L; NF, normal skin fibroblast; ns, not significant.

Figure 4. Lactate enhances collagen expression, proliferation, and migration via H3K18la-dependent induction of LTBP3 in keloid fibroblasts. (a) The expression of COL1A1, COL1A2, and LTBP3 in KFs after LTBP3 silencing and lactate (20 mM) treatment was examined by qPCR. (b) The expression of collagen-I and LTBP3 in KFs after LTBP3 silencing and lactate (20 mM) treatment was evaluated using Western blotting. (c, d) The proliferation of KFs after LTBP3 silencing and lactate (20 mM) treatment was evaluated using CCK-8 and EdU incorporation assays. The brightness and contrast were adjusted uniformly within each channel. Bar: 200 μm. (e) The migration of KFs after LTBP3 silencing and lactate (20 mM) treatment was evaluated

using Transwell assay. Bar: 200 μm. *$P<0.05$, **$P<0.01$, ***$P<0.001$. CCK-8, Cell Counting Kit 8; EdU, 5-ethynyl-2'-deoxyuridine; h, hour; KF, keloid fibroblast; mM, mmol/L; NF, normal skin fibroblast; OD, optical density; siNC, negative control targeted small interfering RNA; siRNA, small interfering RNA.

Figure 5. Lactate potentiates collagen expression, proliferation, and migration through H3K18la/LTBP3-dependent induction of TGF-β1 secretion in keloid fibroblasts. (a) TGF-β1 levels in KFs after LTBP3 silencing and lactate treatment (20 mM) were measured by ELISA. (b) TGF-β1 levels in KFs overexpressing H3 or its K18R mutant following lactate (20 mM) treatment were measured by ELISA. (c) TGF-β1 levels in KFs treated with oxamate (0-20 mM) for 48 h were measured by ELISA. (d, e) Collagen-I expression in KFs treated with 1D11 (10 μg/ml) and then treated with lactate (20 mM) was examined by qPCR and Western blotting. (f, g) The proliferation of KFs treated with 1D11 (10 μg/ml) and then treated with lactate (20 mM) was evaluate using CCK-8 and EdU incorporation assays. The brightness and contrast were adjusted uniformly within each channel. Bar: 200 μm. (h) The migration of KFs treated with 1D11 (10 μg/ml) and then treated with lactate (20 mM) was evaluated using Transwell assay. Bar: 200 μm. *$P<0.05$, ***$P<0.001$. CCK-8, Cell Counting Kit 8; EdU, 5-ethynyl-2'-deoxyuridine; h, hour; KF, keloid fibroblast; mM, mmol/L; ns, not significant; OD, optical density.

Figure 6. TGF-β1 increases lactate and H3K18 lactylation levels in keloid fibroblasts. (a) Colorimetric assays measuring lactate levels in KFs treated with 1D11

(0-10 μg/ml) for 24 h. (b) Western blotting analysis of collagen-I, PanKla and H3K18la in KFs treated with 1D11 (0-10 μg/ml) for 48 h. (c) Colorimetric assays measuring lactate levels in KFs treated with TGF-β1 (0-10 ng/ml) for 24 h. (d) Western blotting analysis of collagen-I, PanKla and H3K18la in KFs treated with TGF-β1 (0-10 ng/ml) for 48 h. (e) In keloid fibroblasts, increased H3K18la levels caused by lactate accumulation increase the transcription of LTBP3, which promotes cell collagen expression, proliferation, and migration through TGF-β1. In turn, TGF-β1 promotes lactate and H3K18 lactylation, thereby forming a lactate/H3K18la/LTBP3/TGF-β1 positive feedback loop. ***P<0.01*, ****P<0.001*. h, hour; KF, keloid fibroblast; ns, not significant.

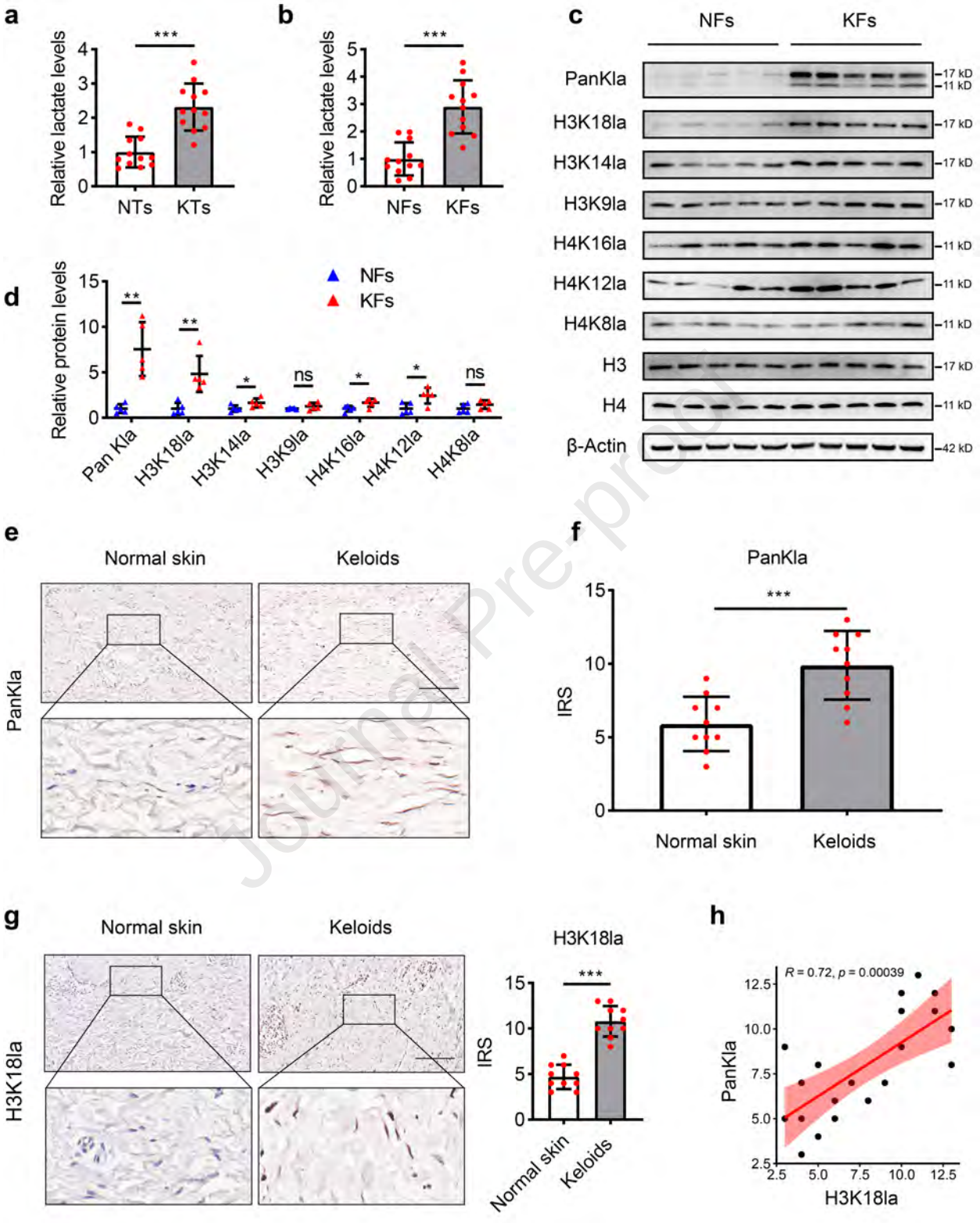

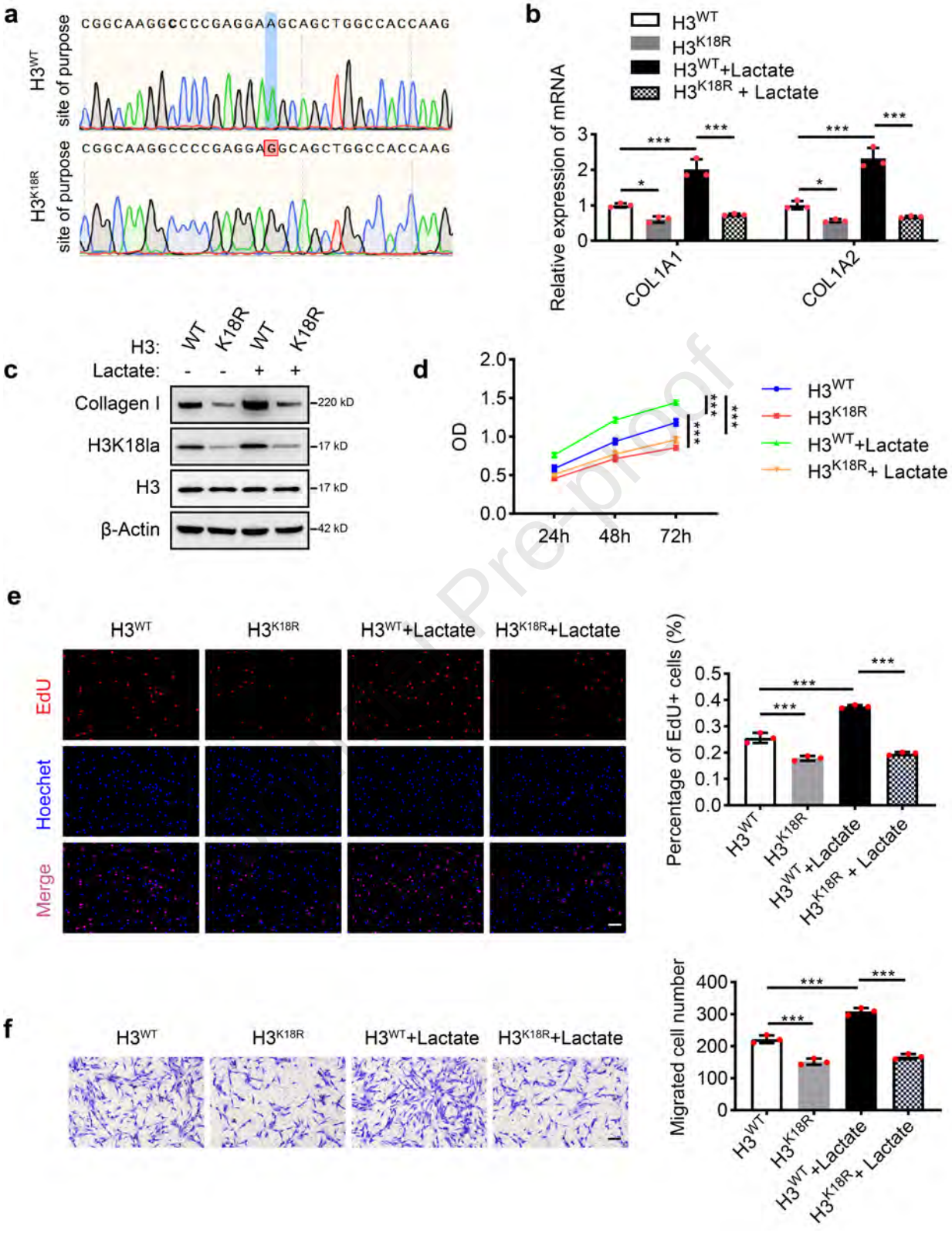
a
H3WT site of purpose
CGGCAAGGCCCCGAGGAAGCAGCTGGCCACCAAG
H3K18R site of purpose
CGGCAAGGCCCCGAGGAGGCAGCTGGCCACCAAG
b
H3WT
H3K18R
H3WT+Lactate
H3K18R + Lactate
Relative expression of mRNA
COL1A1
COL1A2
c
H3:
Lactate:
Collagen I
H3K18la
H3
β-Actin
220 kD
17 kD
17 kD
42 kD
d
OD
24h
48h
72h
H3WT
H3K18R
H3WT+Lactate
H3K18R+ Lactate
e
H3WT
H3K18R
H3WT+Lactate
H3K18R+Lactate
EdU
Hoechet
Merge
Percentage of EdU+ cells (%)
f
Migrated cell number

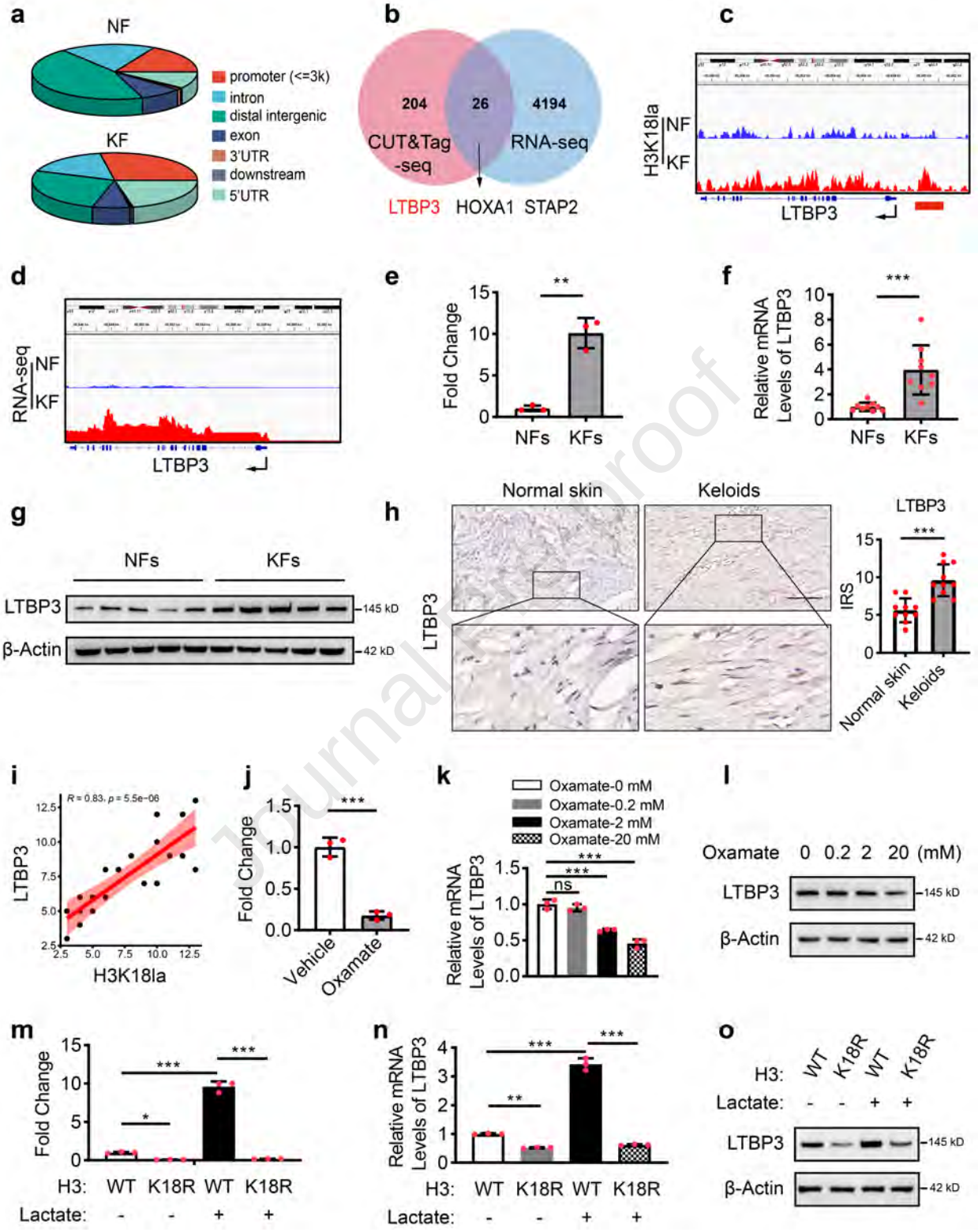
a
NF
KF
promoter (<=3k)
intron
distal intergenic
exon
3'UTR
downstream
5'UTR
b
204
26
4194
CUT&Tag -seq
RNA-seq
LTBP3
HOXA1
STAP2
c
H3K18la
NF
KF
LTBP3
d
RNA-seq
NF
KF
LTBP3
e
Fold Change
NFs
KFs
f
Relative mRNA Levels of LTBP3
NFs
KFs
g
NFs
KFs
LTBP3
145 kD
β-Actin
42 kD
h
Normal skin
Keloids
LTBP3
IRS
Normal skin
Keloids
i
R = 0.83, p = 5.5e-06
LTBP3
H3K18la
j
Fold Change
Vehicle
Oxamate
k
Oxamate-0 mM
Oxamate-0.2 mM
Oxamate-2 mM
Oxamate-20 mM
Relative mRNA Levels of LTBP3
ns
l
Oxamate 0 0.2 2 20 (mM)
LTBP3
145 kD
β-Actin
42 kD
m
Fold Change
H3: WT K18R WT K18R
Lactate: - - + +
n
Relative mRNA Levels of LTBP3
H3: WT K18R WT K18R
Lactate: - - + +
o
H3: WT K18R WT K18R
Lactate: - - + +
LTBP3
145 kD
β-Actin
42 kD

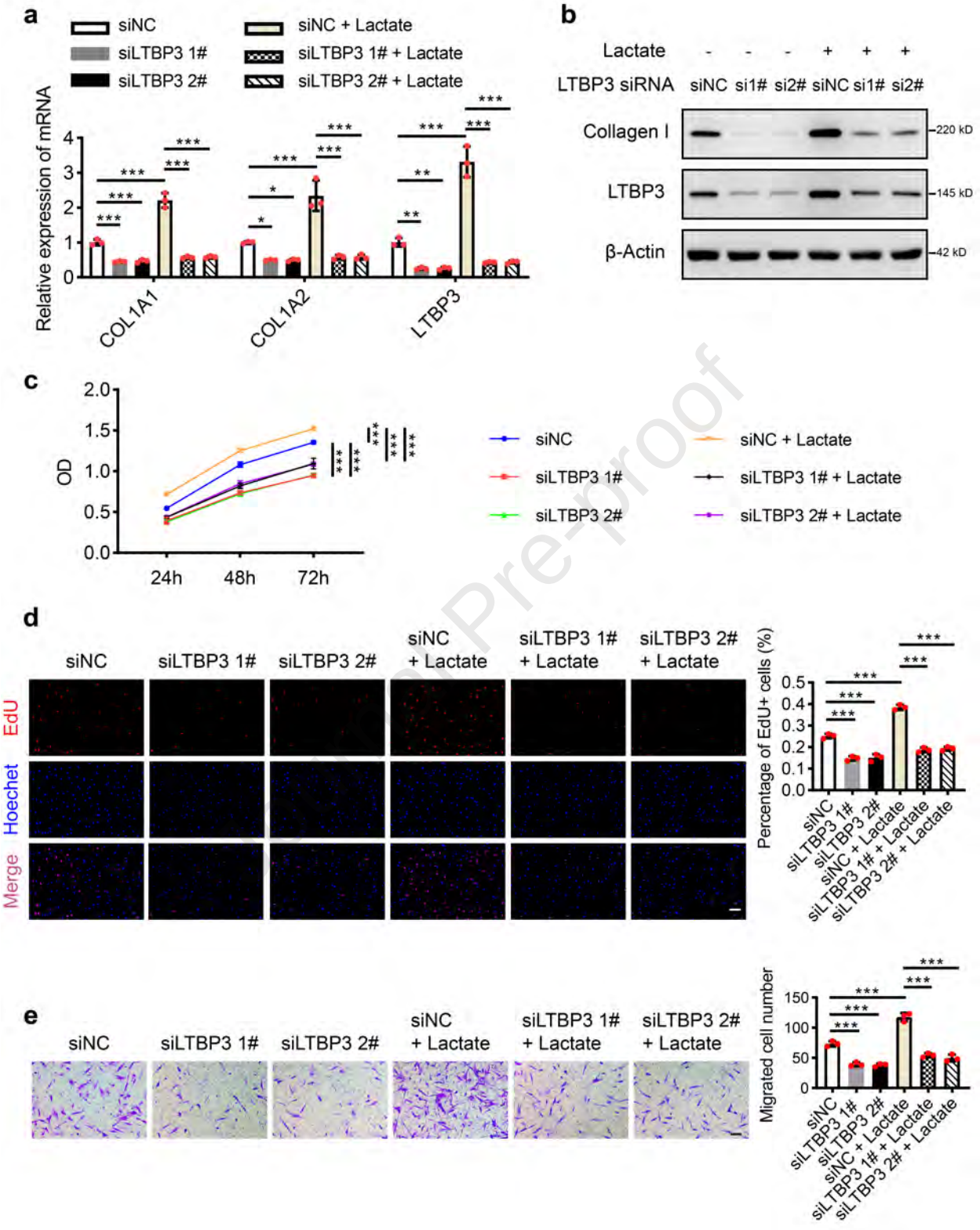

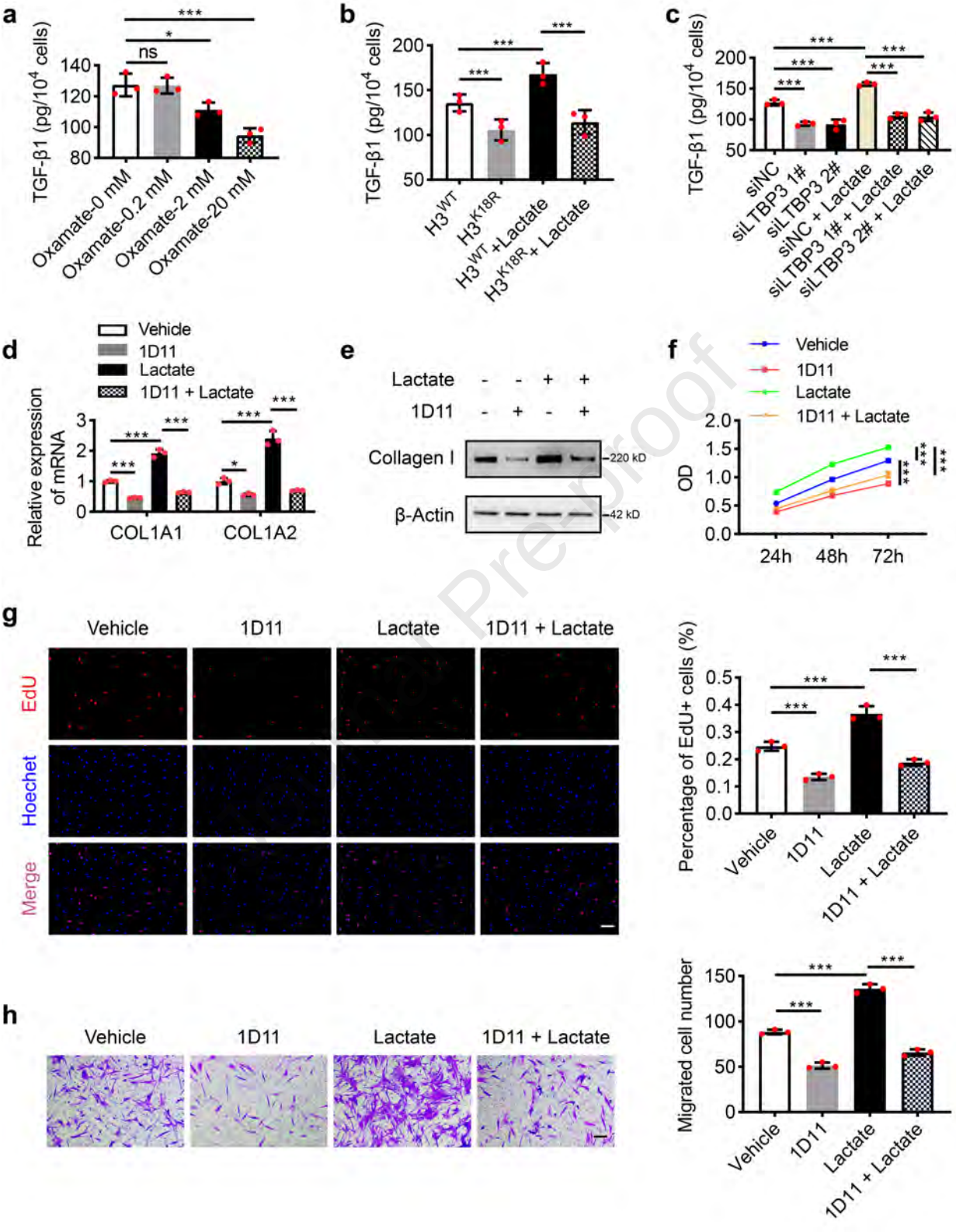
a
TGF-β1 (pg/10^4 cells)
Oxamate-0 mM
Oxamate-0.2 mM
Oxamate-2 mM
Oxamate-20 mM
b
TGF-β1 (pg/10^4 cells)
H3^WT
H3^K18R
H3^WT +Lactate
H3^K18R + Lactate
c
TGF-β1 (pg/10^4 cells)
siNC
siLTBP3 1#
siLTBP3 2#
siNC + Lactate
siLTBP3 1# + Lactate
siLTBP3 2# + Lactate
d
Vehicle
1D11
Lactate
1D11 + Lactate
Relative expression of mRNA
COL1A1
COL1A2
e
Lactate
1D11
Collagen I
β-Actin
220 kD
42 kD
f
Vehicle
1D11
Lactate
1D11 + Lactate
OD
24h
48h
72h
g
Vehicle
1D11
Lactate
1D11 + Lactate
EdU
Hoechet
Merge
Percentage of EdU+ cells (%)
h
Vehicle
1D11
Lactate
1D11 + Lactate
Migrated cell number

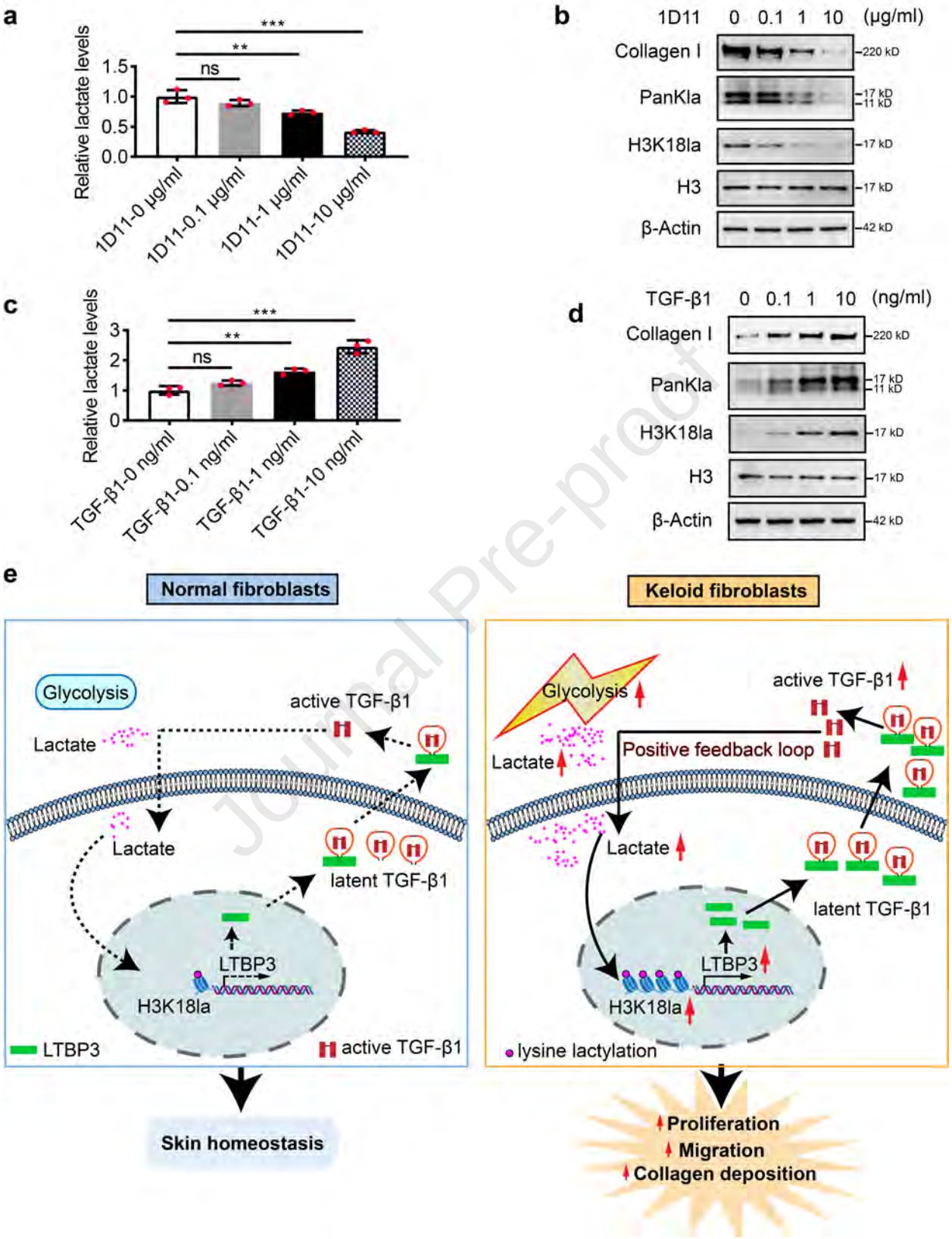

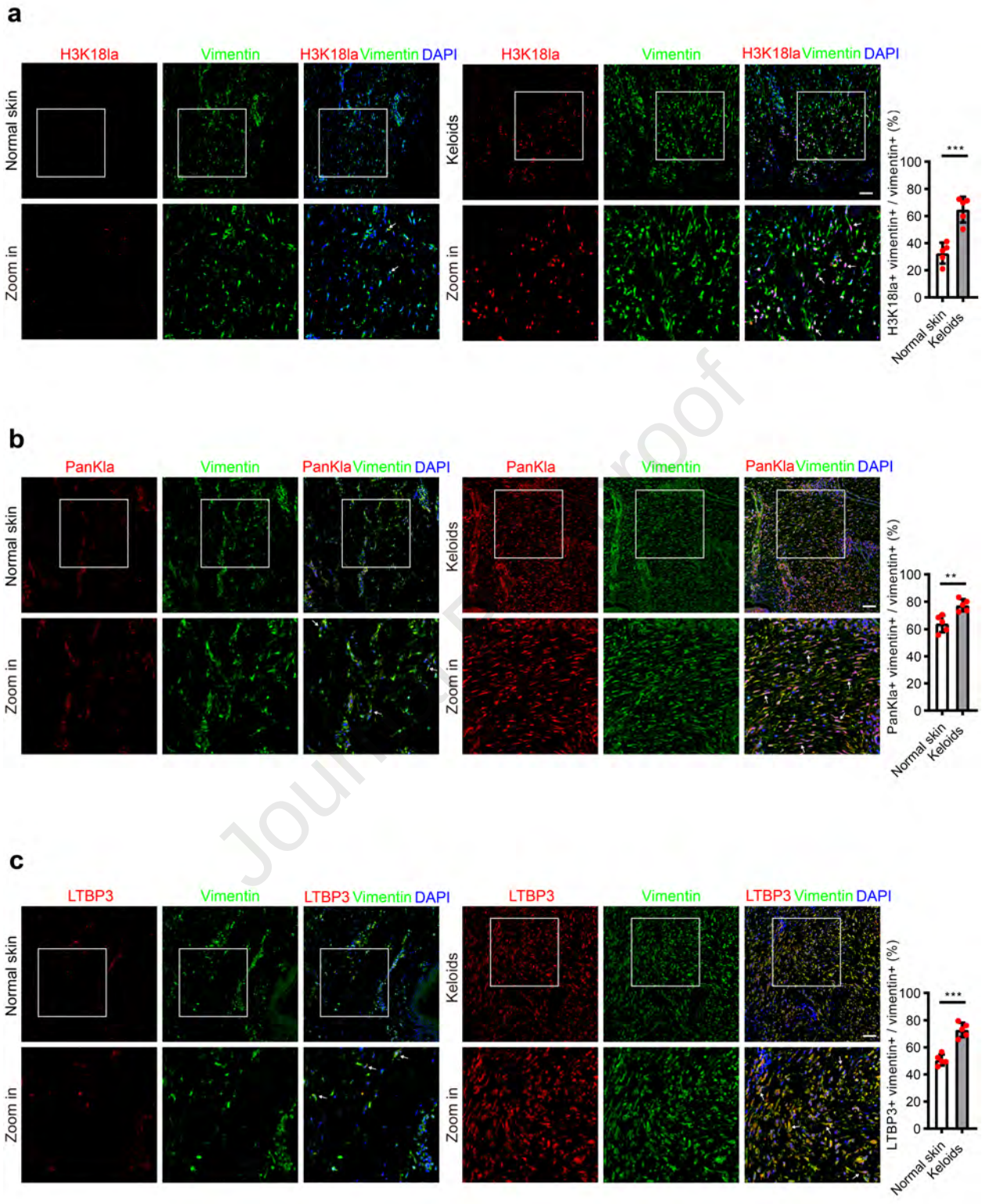

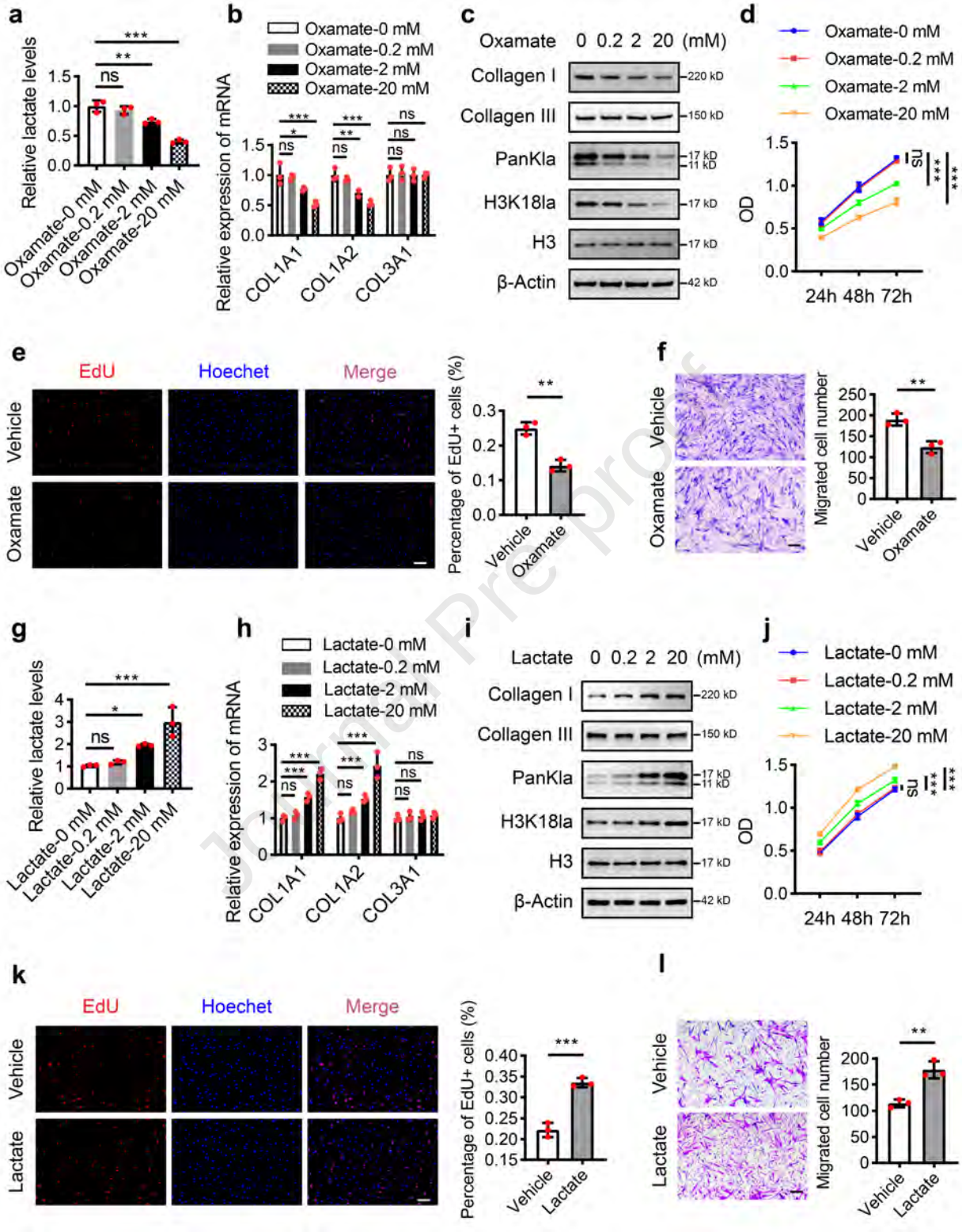

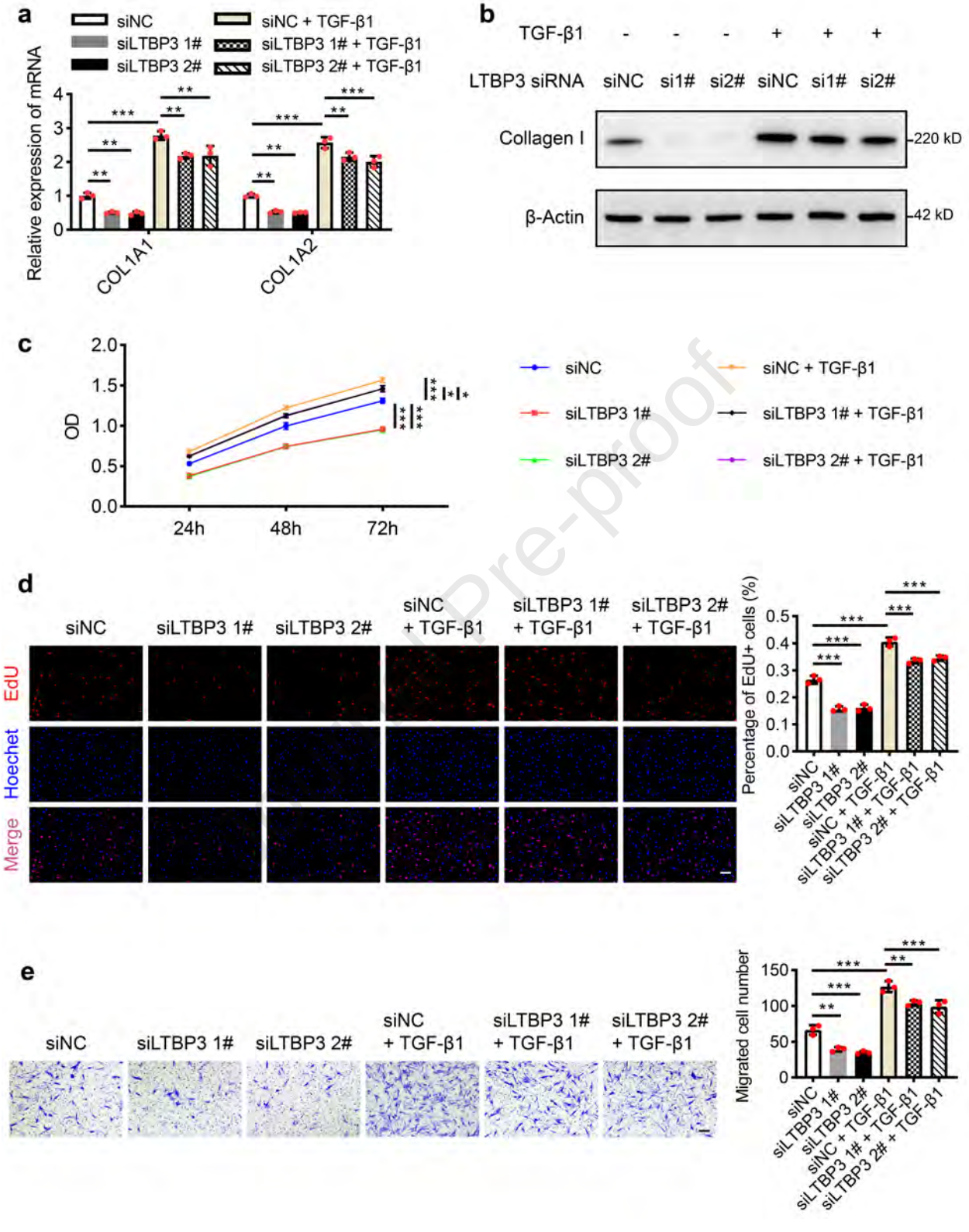
a
siNC
siLTBP3 1#
siLTBP3 2#
siNC + TGF-β1
siLTBP3 1# + TGF-β1
siLTBP3 2# + TGF-β1
Relative expression of mRNA
COL1A1
COL1A2
b
TGF-β1
LTBP3 siRNA
siNC
si1#
si2#
Collagen I
β-Actin
220 kD
42 kD
c
OD
24h
48h
72h
d
EdU
Hoechet
Merge
Percentage of EdU+ cells (%)
e
Migrated cell number

Supplementary materials and methods

Western blotting

Proteins were extracted from the cells via RIPA lysis buffer (Beyotime, Haimen, China) supplemented with protease inhibitor cocktails (Beyotime, Haimen, China). Protein samples were separated by SDS-PAGE and then transferred to polyvinylidene difluoride membranes (Millipore, MA, USA). After blocking with 5% skim milk, the membranes were incubated with primary antibodies overnight at 4°C and then with HRP-conjugated secondary antibodies for 1 h at room temperature. Next, the protein bands were detected with a Chemiluminescence instrument (Bio-Rad, CA, USA) and quantified with ImageJ software. The primary antibodies against PanKla (PTM-1401RM), H3 (PTM-1002RM), H4 (PTM-1015RM), H3K18la (PTM-1427RM), H3K14la (PTM-1414RM), H3K9la (PTM-1419RM), H4K16la (PTM-1417RM), H4K12la (PTM-1411RM), H4K8la (PTM-1415RM), and β-Actin (PTM-5028) were purchased from PTM Bio, Inc. (Hangzhou, China); Antibodies against collagen I (ab138492) and collagen III (ab184993) were obtained from Abcam (Cambridge, MA, USA); and an antibody against LTBP3 (ABT316) was acquired from Sigma–Aldrich (St. Louis, MO, USA).

RNA extraction and real-time quantitative PCR (RT-qPCR)

RNA was isolated with TRIzol reagent (Invitrogen, Carlsbad, CA, USA) following the manufacturer's guidelines. A cDNA kit (Takara, Tokyo, Japan) was used for reverse transcription. RT-qPCR was performed utilizing SYBR Green Master Mixes (Vazyme,

Nanjing, China), on a Bio-Rad real-time PCR detection system following the provided guidelines. The qPCR primers used in this research are listed in Table S2. The relative mRNA expression levels were calculated using the comparative Ct method, and the results were normalized to endogenous β-actin levels.

Cell transfection with siRNA

Specific siRNAs targeting LTBP3 and nontargeting control siRNAs were purchased from Ribo Bio. (Guangzhou, China). These siRNAs were then transfected into skin fibroblasts using RNAiMAX (Invitrogen, CA, USA) following the guidelines provided by the manufacturer.

Lentiviral transduction

For lentiviral infection of keloid fibroblasts, cells were seeded into a 6-well plate (6×10^5 cells/well) and infected with lentivirus (Hanheng Biotechnology, Shanghai, China) at a multiplicity of infection (MOI) of 25 in the presence of 8 μg/mL polybrene (Hanheng Biotechnology, Shanghai, China). Stable cells were selected with complete medium supplemented with 2 μg/mL puromycin (Hanheng Biotechnology, Shanghai, China) and confirmed by Western blotting.

Immunohistochemistry (IHC)

Keloid and normal skin tissues were fixed in 4% paraformaldehyde for 24 h and then embedded in paraffin. The samples were sectioned (5 μm-thick), and then the tissue

sections were deparaffinized, hydrated, and subjected to antigen retrieval. Next, 3% H_2O_2 was used to block endogenous peroxidase activity. The tissue sections were incubated with primary antibodies overnight at 4°C. The following primary antibodies were used in this study: rabbit anti-PanKla (PTM-1401RM) and rabbit anti-H3K18la (PTM-1406RM), purchased from PTM Bio Inc (Hangzhou, China), and rabbit anti-LTBP3 (ABT316), purchased from Sigma-Aldrich (St Louis, MO, USA). After incubation with HRP-conjugated secondary antibodies, the tissue sections were stained with 3,3′-diaminobenzidine (DAB) reagent and hematoxylin. Finally, an Envision System (Dako, CA, USA) was used to capture images.

The IHC results were analyzed semiquantitatively by two independent researchers, who were blinded to the experimental groups, via the immunoreactivity score (IRS) method as previously described (Gu et al., 2023, Hu et al., 2017). The IRS value ranges from 0 to 12, and it was calculated by multiplying the percentage of positive cells (1: ≤25%; 2: 26–50%; 3: 51–74%; 4: ≥75%) by the staining intensity (0: negative; 1: weak; 2: moderate; 3: strong). The average value from the two researchers was the final score. Multivariate logistic regression modeling was subsequently performed to statistically correlate the clinical parameters with the IRS results.

Immunofluorescence staining

Keloid and normal skin tissues were fixed in 4% paraformaldehyde for 24 h and then embedded in paraffin. The samples were sectioned (5 μm-thick) and the tissue sections were then deparaffinized, hydrated, subjected to antigen retrieval and blocked

in 10% bovine serum albumin (Thermo Fisher Scientific, MA, USA). Next, the tissue sections were incubated with primary antibodies overnight at 4°C. The following primary antibodies were used in this study: rabbit anti-PanKla (PTM-1401RM) and rabbit anti-H3K18la (PTM-1406RM), purchased from PTM Bio Inc (Hangzhou, China); rabbit anti-LTBP3 (ABT316), purchased from Sigma-Aldrich (St Louis, MO, USA); and mouse anti-vimentin (60330-1-lg), purchased from Proteintech (Chicago, IL). The next day, all the slides were labeled with two secondary antibodies (goat anti-rabbit and goat anti-mouse) purchased from Abcam at room temperature for 1 h, after which coverslips with DAPI-containing aqueous mounting medium were placed on the slides. Finally, a Nikon A1+ confocal laser-scanning microscope was used to capture images.

Lactate measurement

Lactate concentrations were determined with a colorimetric assay kit (E-BC-K044-M) from Elabscience Bio. (Wuhan, China) following the guidelines provided by the manufacturer.

Enzyme-linked immunosorbent assay (ELISA)

Quantikine ELISA kits (DB100B) purchased from R&D Systems were used to measure TGF-β1 levels following the guidelines provided by the manufacturer.

RNA sequencing and bioinformatics analysis

The mRNA library was prepared from total RNA isolated from skin fibroblasts. The RNA-Seq and initial bioinformatics services used were provided by GENEWIZ, Inc. (Suzhou, China). DESeq2 was used to analyze the differential expression of 3 NFs and 3 KFs, with significance defined by a *P* value < 0.05 and an abs (log2FC) > 0.58. Venn diagrams were created using the R programming language.

Cleavage under targets and tagmentationassay sequencing (CUT&Tag-seq) and qPCR (CUT&Tag-qPCR)

For CUT&Tag-seq, the DNA libraries were sequenced on the Illumina NovaSeq system at GENEWIZ, Inc. Bowtie2 was used to align the clean reads to the human reference genome hg38, MACS2 was used to call narrow peaks, and edgeR was employed to analyze differential peaks between samples. The following thresholds were applied: *P* value < 0.05 and abs (log2FC) > 0.58.

For CUT&Tag-qPCR, the DNA spike-in was used as a reference. The qPCR primers used for spike-in are F: 5'-TCGGTGTGAATCCCATCAGC-3', R: 5'-GCTTATGCTTGCCGACATGG-3'. The qPCR primers used for LTBP3 promoter are F: 5'-AGTCACACCTGTGGGCATCT-3', R: 5'-CCACTACACCTTCGGCTCTC-3'.

5-Ethynyl-2'-deoxyuridine (EdU) incorporation assay

Skin fibroblasts were placed in 24-well plates ($3*10^4$ cells per well), and 24 h later, an EdU incorporation assay was conducted using a commercial kit purchased from Beyotime (Haimen, China) following the provided guidelines. The proportion of EdU-

positive cells = EdU-positive cell count/total cell count × 100%.

Cell Counting Kit-8 (CCK-8) assay

Skin fibroblasts were placed in 96-well plates ($1*10^4$ cells per well) and treated with the corresponding reagents for 24, 48, or 72 h. Subsequently, CCK-8 assay kits purchased from Absin (Beijing, China) were used to examine fibroblast proliferation following the manufacturer's protocols.

Transwell assay

Briefly, after being resuspended in 200 μL of serum-free medium, skin fibroblasts were reseeded in the top chamber (Corning Falcon, NY, USA), and 600 μL of medium supplemented with 10% FBS was added to the lower chamber. The transferred fibroblasts were treated with methanol, stained with crystal violet, and enumerated via an optical microscopy.

Supplemrntary references

Gu JJ, Deng CC, Feng QL, Liu J, Zhu DH, Cheng Q, et al. Relief of Extracellular Matrix Deposition Repression by Downregulation of IRF1-Mediated TWEAK/Fn14 Signaling in Keloids. J Invest Dermatol 2023;143(7):1208-19.e6.

Hu ZC, Shi F, Liu P, Zhang J, Guo D, Cao XL, et al. TIEG1 Represses Smad7-Mediated Activation of TGF-β1/Smad Signaling in Keloid Pathogenesis. J Invest Dermatol 2017;137(5):1051-9.

Supplementary table

Supplementary Table S1. Basic information of subjects involved in the research.

No.	Age (y)	Gender	Diagnosis	Site of Sampling	No.	Age (y)	Gender	Site of Sampling
K 1[1,3]	50	F	keloid	Back	N 1[2]	17	M	Ear
K 2[2,4,6]	21	M	keloid	Chest	N 2[2,5]	46	M	Face
K 3[1,2,4]	19	F	keloid	Ear	N 3[2,3]	33	F	Back
K 4[3]	26	F	keloid	Ear	N 4[2]	52	F	Back
K 5[1,2,5]	25	M	keloid	Chest	N 5[2,3,4]	29	M	Back
K 6[1,2,4]	27	M	keloid	Shoulder	N 6[1,2,4]	43	F	Abdomen
K 7[3]	29	F	keloid	Back	N 7[1]	36	M	Back
K 8[1]	21	F	keloid	Back	N 8[1]	30	M	Back
K 9[2,6]	23	M	keloid	Back	N 9[2,4]	35	M	Thigh
K 10[1,2,6]	56	F	keloid	Chest	N 10[3]	24	F	Abdomen
K 11[2,5]	33	F	keloid	Ear	N 11[1,3]	41	M	Abdomen
K 12[1,2,4]	52	M	keloid	Thigh	N 12[3]	37	F	Chest
K 13[1,2]	18	M	keloid	Chest	N 13[2,3]	25	F	Back
K 14[1]	34	M	keloid	Thigh	N 14[1,3]	47	M	Back
K 15[1,2]	28	M	keloid	Chest	N 15[1,3]	25	F	Chest
K 16[3]	27	F	keloid	Shoulder	N 16[3]	24	F	Thigh
K 17[1,3]	25	F	keloid	Chest	N 17[1,2]	53	F	Upper arm
K 18[2,4,6]	37	F	keloid	Abdomen	N 18[1,3]	24	M	Thigh
K 19[3]	29	F	keloid	Back	N 19[1,2]	29	F	Thigh
K 20[2,5]	23	M	keloid	Shoulder	N 20[2]	22	F	Upper arm
K 21[3]	28	F	keloid	Back	N 21[1,2,4,5]	26	M	Upper arm
K 22[3]	27	M	keloid	Chest	N 22[1]	30	M	Back
K 23[3]	25	F	keloid	Abdomen	N 23[2,4,5]	28	F	Shoulder
K 24[3]	32	M	keloid	Shoulder	N 24[1]	25	M	Chest
K 25[1,2,6]	17	F	keloid	Ear				

[1] Lactate levels were determined in fresh tissues.
[2] Fresh biopsy tissues were utilized to isolate primary fibroblast, and the cell strains were used to determine lactate levels.
[3] Paraffin sections were used in immunohistochemistry or immunofluorescent staining.
[4] Cell strains were used to assess histone lactylation (Figure 1c, 1d) and LTBP3 (Figure 3g) protein levels.
[5] Cell strains were used in RNA-sequencing, CUT&Tag-sequencing or CUT&Tag-qPCR.
[6] Cell strains were used in cell experiments (qPCR, western blotting, CCK-8, EdU, Transwell)

Abbreviations: CCK-8, Cell Counting Kit 8; EdU, 5-ethynyl-2'-deoxyuridine; F, female; M, male; No, number; K, keloid; N, normal.

Supplementary Table S2. Primer sequences utilized in qPCR analysis.

Gene	Forward Primer (5′→3′)	Reverse Primer (5′→3′)
COL1A1	TGTGCGATGACGTGATCTGTGA	CTTGGTCGGTGGGTGACTCTG
COL1A2	ATGCCTAGCAACATGCCAATC	CAGCAAAGTTCCCACCGAGA
COL3A1	GGAGCTGGCTACTTCTCGC	GGGAACATCCTCCTTCAACAG
LTBP3	TCTACCCCTGCCCAGTCTAC	TCCTTGCAAATCTCCGACCC
β-Actin	AGAGCTACGAGCTGCCTGAC	AGCACTGTGTTGGCGTACAG

Supplementary Table S3. The oligonucleotides Sequence of small interfering RNA.

Name	Sequence (5′- 3′)
LTBP3 siRNA	ACAACAACATCGTCAACTA
	GGAGGATTCAGACGAGTGT

Supplementary Figure legends

Supplementary Figure S1. Immunofluorescence staining of H3K18la, PanKla, LTBP3 and vimentin in normal and keloid tissues. (a) Representative images of immunofluorescence staining of H3K18la (red) and Vimentin (green) in NTs and KTs (n=5 per group). The white arrows indicate H3K18la+/Vimentin+ cells. The percentage of H3K18la+/Vimentin+ cells among the Vimentin-labeled cells was quantified. Bar: 200 μm. (b) Representative images of immunofluorescence staining of PanKla (red) and Vimentin (green) in NTs and KTs (n=5 per group). The white arrows indicate PanKla+/Vimentin+ cells. The percentage of PanKla+/Vimentin+ cells among the Vimentin-labeled cells was quantified. Bar: 200 μm. (c) Representative images of

immunofluorescence staining of LTBP3 (red) and Vimentin (green) in NTs and KTs (n=5 per group). The white arrows indicate LTBP3+/Vimentin+ cells. The percentage of LTBP3+/Vimentin+ cells among the Vimentin-labeled cells was quantified. Bar: 200 μm. ***P<0.01*, ****P<0.001*. KT, keloid tissue; NT, normal skin tissue.

Supplementary Figure S2. Lactate promotes keloid fibroblast collagen expression, proliferation, and migration with increased histone lactylation. (a) Colorimetric assays measuring lactate levels in KFs treated with oxamate (0-20 mM) for 24 h. (b) The mRNA levels of COL1A1, COL1A2, and COL3A1 in KFs treated with oxamate (0-20 mM) for 48 h. (c) Western blotting analysis of collagen-I, collagen-III, PanKla and H3K18la in KFs treated with oxamate (0-20 mM) for 48 h. (d) The proliferation of KFs treated with oxamate (0-20 mM) was evaluated using CCK-8 assay. (e) The proliferation of KFs treated with oxamate (20 mM) treatment for 48 h was evaluated using EdU incorporation assay. The brightness and contrast were adjusted uniformly within each channel. Bar: 200 μm. (f) The migration of KFs treated with oxamate (20 mM) for 48 h was evaluated using Transwell assay. Bar: 200 μm. (g) Lactate levels in KFs treated with lactate (0-20 mM) for 24 h. (h) The mRNA levels of COL1A1, COL1A2, and COL3A1 in KFs treated with lactate (0-20 mM) for 48 h. (i) Western blotting analysis of collagen-I, collagen-III, PanKla and H3K18la in KFs treated with lactate (0-20 mM) for 48 h. (j) The proliferation of KFs treated with lactate (0-20 mM) was evaluated using CCK-8 assay. (k) The proliferation of KFs treated with lactate (20 mM) for 48 h was evaluated using EdU incorporation assay. The brightness and contrast

were adjusted uniformly within each channel. Bar: 200 μm. (l) The migration of KFs treated with lactate (20 mM) for 48 h was evaluated using Transwell assay. Bar: 200 μm. *$P<0.05$, **$P<0.01$, ***$P<0.001$. CCK-8, Cell Counting Kit 8; EdU, 5-ethynyl-2'-deoxyuridine; h, hour; KF, keloid fibroblast; mM, mmol/L; ns, not significant; OD, optical density.

Supplementary Figure S3. LTBP3 promotes collagen expression, proliferation, and migration through TGF-β1 in keloid fibroblasts. (a, b) Collagen-I expression in KFs transfected with LTBP3 siRNA and treated with TGF-β1 (10 ng/ml) was evaluated using qPCR and Western blotting. (c, d) The proliferation of KFs transfected with LTBP3 siRNA transfection and treated with TGF-β1 (10 ng/ml) was evaluated using CCK-8 and EdU incorporation assays. The brightness and contrast were adjusted uniformly within each channel. Bar: 200 μm. (e) The migration of KFs transfected with LTBP3 siRNA and treated with TGF-β1 (10 ng/ml) was evaluated using Transwell assay. Bar: 200 μm. *$P<0.05$, **$P<0.01$, ***$P<0.001$. CCK-8, Cell Counting Kit 8; EdU, 5-ethynyl-2'-deoxyuridine; h, hour; KF, keloid fibroblast; mM, mmol/L; OD, optical density.